DOI: 10.1002/ejic.200700584

Synthesis, Crystal Structures, and Photophysical Properties of Lanthanide Complexes Containing Pyrrole-Derivatized Carboxylate Ligands

Ga-Lai Law,[a] Ka-Leung Wong,[b] Kok-Kin Lau,[a] Hoi-Lam Tam,[c] Kok-Wai Cheah,[c] and Wing-Tak Wong*[a]

Keywords: Lanthanide / Luminescence / Terbium / Europium / Pyrrole

Two pyrrole-deriviatized carboxylic acids [$\mathbf{L^1}$ = 1-methylpyrrole-2-carboxylate] and [$\mathbf{L^2}$ = *N*-methyl-3-indoleglyoxylate] were used as ligands to prepare six lanthanide coordination compounds $[(\mathbf{L^1})_3Ln]_n$ (Ln = Eu, **1**; Gd, **2**; Tb, **3**) and $[(\mathbf{L^2})_n$-$Ln(NO_3)(MeOH)_2]_n$ (Ln = Eu, **4**; Gd, **5**; Tb, **6**). These complexes have been synthesized and structurally characterized by single-crystal X-ray diffraction. The phosphorescence behavior of the ligands in the Gd^{3+} complexes show that modification of the ligands can tune the triplet energy levels of the ligands so that they match the $^5D_0$ energy level of Eu^{3+} and the $^5D_4$ energy level of Tb^{3+}; thus, the energy transfer efficiency from antenna to Eu^{3+} and Tb^{3+} is improved, and the Eu^{3+} and Tb^{3+} emission intensity is enhanced. This concept can be applied towards improving the luminescent properties of Ln^{3+} complexes by the modification of coordinating ligands.

Introduction

One topic of current interest in materials research is the synthesis of lanthanide complexes because of their promising photoluminescent properties. The major advantages of lanthanide complexes as luminescent materials are the long emission lifetimes and narrow bandwidths.[1–3] Because lanthanide f–f transitions are Laporte forbidden, the direct excitation of electrons in lanthanide-metal ions is very inefficient; thus, the resulting emissions from lanthanide-metal ions are very weak.[4–6] One way to improve the weak luminescence properties of lanthanide ions is to use sensitizing chromophores or antennae as ligands in lanthanide-metal complexes.[7–8] Through complexation with a chromophore, the luminescence of the lanthanide ions can be enhanced greatly (by more than 10^4 fold).[9] This enhancement is mainly because direct excitation of the lanthanide ions can be avoided. In other words, luminescence in lanthanide–ligand complexes results from the electronic excitation of the coordinated chromophore followed by ligand-to-lanthanide energy transfer.

The choice of ligand for complexation plays a key role in constructing efficient luminescent lanthanide complexes. Two common requirements for selecting a ligand for coordination with lanthanide ions are the metal binding strength and ultraviolet (UV) absorption properties of the ligand. Among several categories of organic ligands, aromatic carboxylate ligands are one of the most common groups that fulfil the above two basic requirements. Aromatic carboxylate ligands are frequently used as sensitizing agents for enhancing the luminescence in the lanthanide species because they can chelate the lanthanide-metal ions tightly through their anionic carboxylate groups and strongly absorb UV radiation; the energy absorbed is subsequently transferred to the lanthanide-metal centre.[10–11]

Herein we report six lanthanide–organic complexes that incorporate two types of carboxylic acid ligands 1-methylpyrrole-2-carboxylate ($\mathbf{L^1}$) and *N*-methyl-3-indoleglyoxylate ($\mathbf{L^2}$) (Figure 1). These ligands are complexed with lanthanide(III) nitrate salts to form [Ln(1-methylpyrrole-2-carboxylate)$_3$(MeOH)$_2$(H_2O)] (Ln = Eu, Gd, and Tb for **1**, **2**, and **3**, respectively) and $[Ln_2$(*N*-methyl-3-indoleglyoxylate$)_6$-$(MeOH)_4]_n$ (Ln = Eu, Gd, and Tb for **4**, **5** and **6**, respectively). Both of $\mathbf{L^1}$ and $\mathbf{L^2}$ show strong antenna effects with high quantum efficiency, and two molecular structures (**1** and **4**) of the newly synthesized complexes have been elucidated in this work.

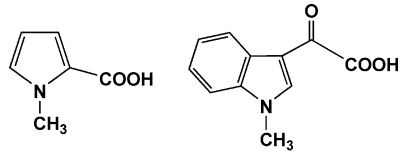

$\mathbf{L^1}$ $\mathbf{L^2}$

Figure 1. The molecular structures of $\mathbf{L^1}$ and $\mathbf{L^2}$.

[a] Department of Chemistry, The University of Hong Kong, Pokfulam, Hong Kong
Fax: +852-2547-2933
E-mail: wtwong@hkucc.hku.hk
[b] Department of Biology and Chemistry, City University of Hong Kong,
TatChee Avenue, Kowloon Tong, Hong Kong
[c] Department of Physics, Hong Kong Baptist University, Kowloon Tong, Hong Kong
Supporting information for this article is available on the WWW under http://www.eurjic.org or from the author.

Results and Discussion

Crystal Structures of 1 and 4

The X-ray diffraction analysis reveals that **1** and **4** adopt a highly symmetrical, polymeric structure in which the europium metal ions form the skeleton. All europium ions in the two europium complexes adopt a nine-coordinate geometry. In **1**, each europium ion is bidentately coordinated by three bidentate carboxylate ligands and monodentately coordinated by another three tridentate, bridging carboxylate ligands. Two of the three tridentate, bridging carboxylate ligands are bidentately chelated to an adjacent europium ion, and the remaining tridentate, bridging carboxylate ligand is bidentately coordinated to another adjacent europium ion (Figure 2). Each europium ion can be described as a nine-coordinate, twisted tricapped trigonal prism, in which the top plane is formed by O(1), O(4), and O(6) atoms, whereas the bottom plane is defined by the other equivalent, but offset in position, O(1), O(4), and O(6) atoms. The O(2), O(3), and O(5) atoms cap three quadrilateral faces of the trigonal prism. The packing diagram of **1** is shown in Figure 3.

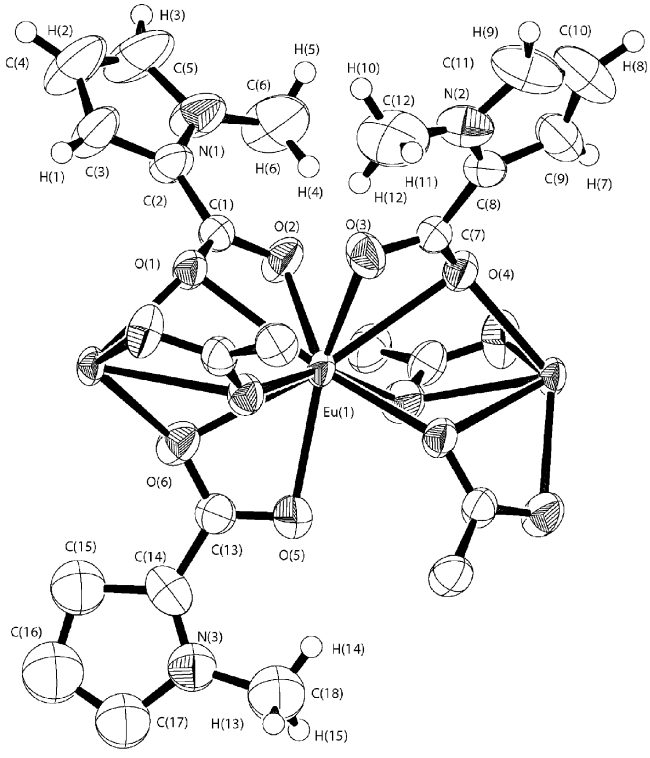

Figure 2. ORTEP drawing of **1**.

The Eu–Eu bond length and Eu–Eu–Eu bond angle in **1** are 3.793 Å and 178.38°, respectively. The bond length is much shorter and the bond angle is much larger than those in $[Eu_2(Benzoate)_6(MeOH)_4]_n$ (4.915 Å and 165.7°). The Eu–O bond lengths in **1** range from 2.400(3) to 2.727(3) Å, which are longer than those of $[Eu_2(Benzoate)_6(MeOH)_4]_n$ [2.309(6) to 2.535(6) Å].[11] The average Eu–O bond length (2.410 Å) for the carboxylate O atoms chelated by only one

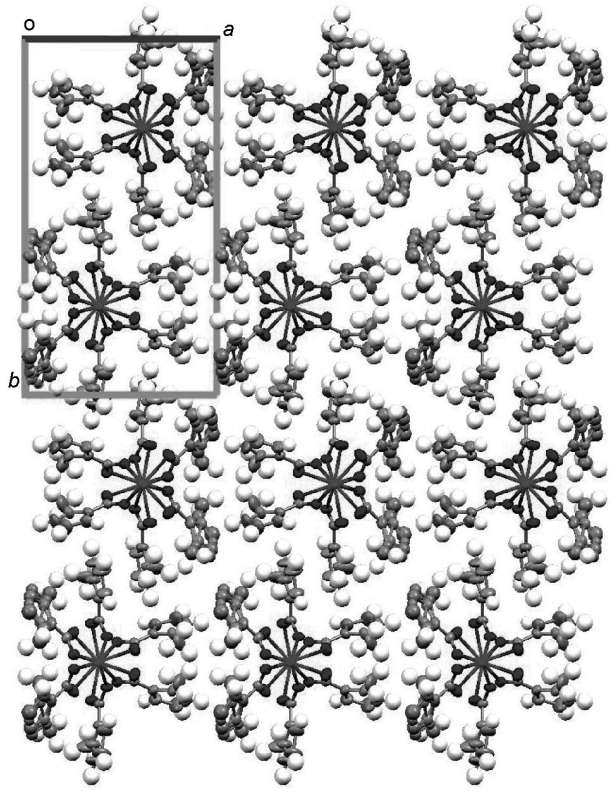

Figure 3. Packing diagram for **1** projected down the *c* axis.

europium ion is shorter than the average Eu–O bond length (2.672 Å) for the carboxylate O atoms chelated by two europium ions, which is obviously because of steric hindrance. The average C–O(CO) distance and O(CO)–C–O(CO) angle are 1.268 Å and 119.6,° respectively. The average C–O–Eu bond angle (88.1°) for the carboxylate O atoms chelated by two europium ions is much smaller than the average C–O–Eu bond angle (101.3°) for the carboxylate O atoms chelated by only one europium ion. The average O(CO)–Eu–O(CO) bond angle is 50.77°.

Recrystallization of the europium complex that contained the glyoxylate ligand gave light yellow, plate-like crystals of **4**, which were studied by X-ray diffraction crystallography. The perspective view of **4** is shown in Figure 4. The packing diagram of **4** projecting down the *a* axis is shown in Figure 5. Summaries of the crystallographic data and experimental parameters for **1** and **4** are supplied in the Supporting Information along with selected bond lengths and angles.

Complex **4** is a polymeric chain, in which europium ions constitute the skeleton. As shown in Figure 4, each europium ion in **4** is nine-coordinate, with five oxygen atoms from three glyoxylate ligands, two oxygen atoms from one nitrate molecule and two oxygen atoms from two methanol solvent molecules. The presence of an additional carbonyl group in glyoxylate ligands relative to that in carboxylate ligands results in an unusual coordination between the glyoxylate ligands and the lanthanide ions. In the structure

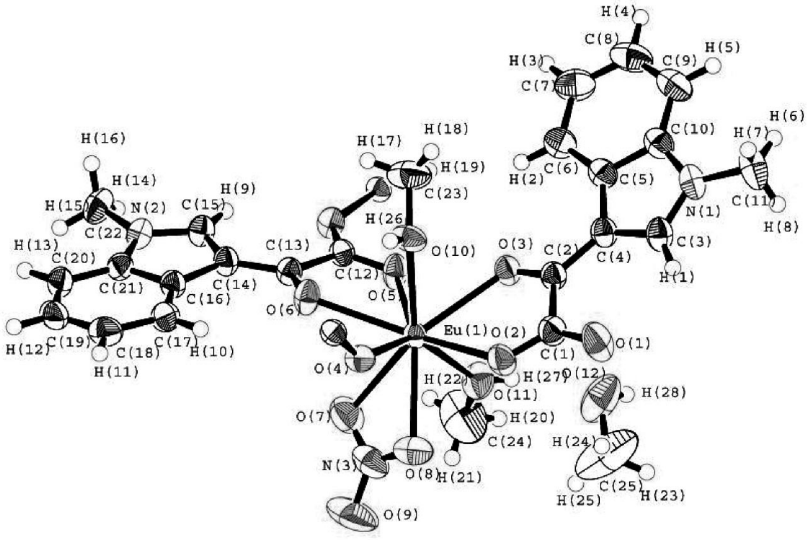

Figure 4. ORTEP drawing of **4**.

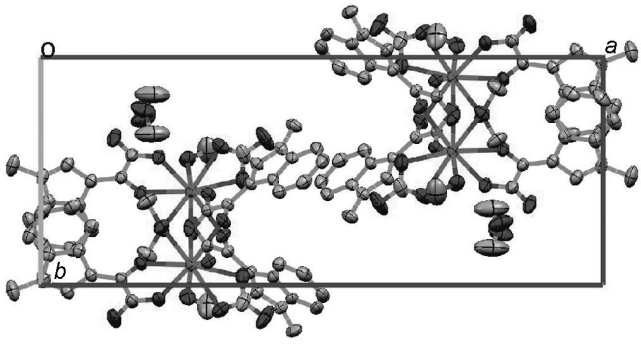

Figure 5. Packing diagram of **4** projected down the *a* axis.

of **4**, each europium ion is coordinated to two carbonyl oxygen atoms of two glyoxylate ligands and three carboxylic oxygen atoms of three glyoxylate ligands. In other words, two carboxylate groups of two or three glyoxylate ligands coordinate as bidentate bridges between two europium ions, whereas the carboxylate group of the remaining glyoxylate ligand coordinates as bidentate bridges between one europium ion and one hydrogen atom of a MeOH molecule. The Eu–Eu bond length and Eu–Eu–Eu bond angle in **4** (6.322 Å and 116.21°, respectively) are much longer and smaller than those in $[Eu_2(Benzoate)_6(MeOH)_4]_n$ (4.915 Å and 165.7°, respectively).[11] The longer Eu–Eu bond in **4** probably results from the greater steric hindrance associated with the *N*-methyl-3-indoleglyoxylate group than the benzoate group. The average Eu–O(carboxyl), Eu–O(carbonyl), Eu–O(MeOH), and Eu–O(nitrate) bond lengths in **4** are 2.405, 2.479, 2.474, and 2.496 Å, respectively. The average C–O (carboxyl and Eu-coordinated) bond length and O(carbonyl)–Eu–O(carboxyl) bond angle are 1.252 Å and 64.3°, respectively. There are four different hydrogen bonds in **4**. Two hydrogen bonds form between the hydrogen atom of one of the coordinated MeOH molecules and the two carboxylic oxygen atoms of one of the coordinated glyoxylate ligands [O(10)–H(26)···O(4) 2.62(5) Å and O(10)–H(26)···O(5)^{i} 1.99(5) Å; i: x, 3/2 – y, 1/2 + z]. The third hydrogen bond is formed between the hydrogen atom of the free MeOH molecule and the non-coordinated carboxylic oxygen atom of one of the glyoxylate ligands [O(12)–H(28)···O(1)^{ii} 1.95(7) Å; ii: x, 1/2 – y, 1/2 + z]. The fourth hydrogen bond is formed between the non-coordinated MeOH molecule and one of the coordinated MeOH molecules [O(11)–H(27)···O(12) 2.01(6) Å].

The different number of carbonyl groups in $\mathbf{L^1}$ and $\mathbf{L^2}$ (Figure 1) should result in structural differences in the corresponding lanthanide complexes. Ligand $\mathbf{L^1}$ has only one carbonyl group so is expected to form Ln^{3+} complexes with four-membered rings, whereas $\mathbf{L^2}$ has two carbonyl groups so is expected to form Ln^{3+} complexes with five-membered rings (Figure 4 and Figure 5).

Photophysical Properties of 1–6

The UV/Vis absorption behavior of ligands $\mathbf{L^1}$ and $\mathbf{L^2}$ and their lanthanide complexes are shown in Figure 6 and Figure 7. The three absorption bands observed for **1**–**3** (see the arrows in Figure 6: ca. 32258 cm^{-1}, ca. 28986 cm^{-1}, and ca. 23256 cm^{-1}) and one band observed for **4**–**6** (Figure 7, ca. 30480 cm^{-1}) are similar to the peaks observed in the UV/Vis spectra of the ligands. By comparison of the UV/Vis spectra for **1**–**6** with that of the ligands, the bands can be attributed to benzyl π–π* transitions, which undergo red shifts of approximately 1000 cm^{-1} upon complexation.[12] Moreover, a very close resemblance is observed between the UV/Vis absorption spectra of **1**–**6** and analogous lanthanide complexes that are coordinated by equivalent ligands.

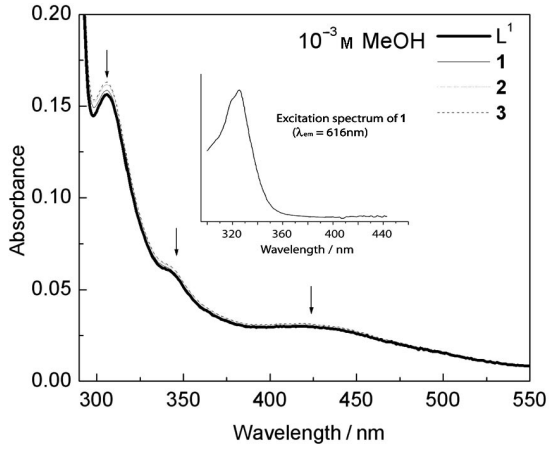

Figure 6. UV/Vis absorption spectra of $\mathbf{L^1}$ and of their complexes **1**–**3**, and the excitation spectra of complex **1** (inset).

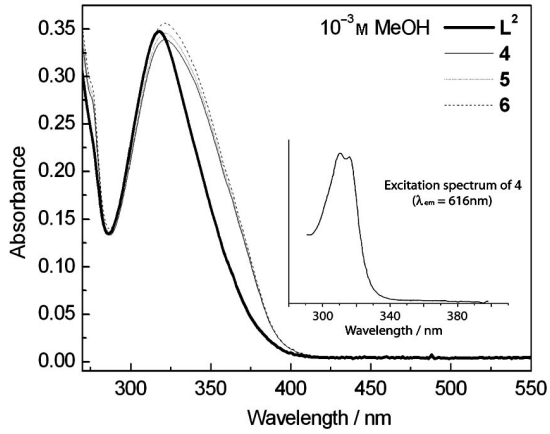

Figure 7. UV/Vis absorption spectra of $\mathbf{L^2}$ and of their complexes **4**–**6**, and the excitation spectra of complex **4** (inset).

The high degree of similarity in the UV/Vis absorption bands of **1**–**6** and those of analogous lanthanide complexes that incorporate equivalent ligands implies that they are likely to have similar or the same ligand–metal coordination modes, and hence similar or the same coordination structure. The slight band broadening observed in the absorption spectra of the complexes **4**–**6** upon complexation is induced by the steric effect of the ligands, which are not equivalent in **4**–**6** (Figure 7).

The luminescence properties of the ligands and of their lanthanide complexes were measured in the solid state at room temperature (Figures 8 and S1). The intense, linear broad emission band (λ_{ex} = 325 nm) characteristic of ligands $\mathbf{L^1}$ and $\mathbf{L^2}$ are shown in the Supporting Information (Figure S1). The emission bands observed for $\mathbf{L^1}$ and $\mathbf{L^2}$ at ca. 400 and 410 nm, respectively, are attributed to the benzyl π–π* relaxation ($S_1 \rightarrow S_0$). The four structured, narrow emission bands at 480, 545, 580, and 620 nm for Tb complexes **3** and **6** and bands at 594, 620, 650 and 700 nm for Eu complexes **1** and **4** are assigned to an electronic energy transition between the $^5D_4 \rightarrow {}^7F_J$ (J = 6, 5, 4, 3) states. The transitions $^5D_0 \rightarrow {}^7F_J$ (J = 1, 2, 3, 4) are shown in the linear process for two types for Tb and Eu complexes.[13] There are great variations between the emission intensity in the Tb and Eu complexes. The matching of the triplet states in these lanthanide systems is an important criteria for the energy transfer from the ligand to the lanthanide (Figure 9 and Figure 10).

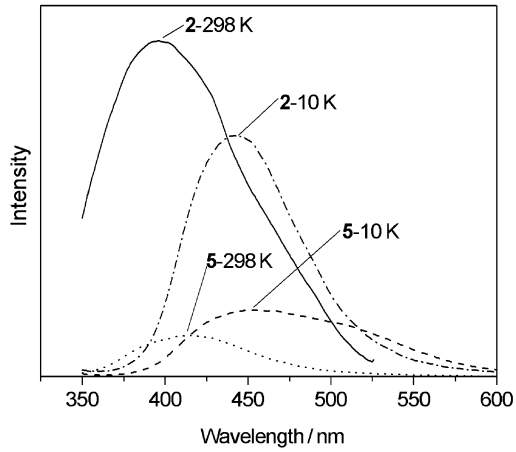

Figure 8. Solid-state emission spectra for Gd complexes **2** and **5** (298 K and 10 K), λ_{ex} = 325 nm.

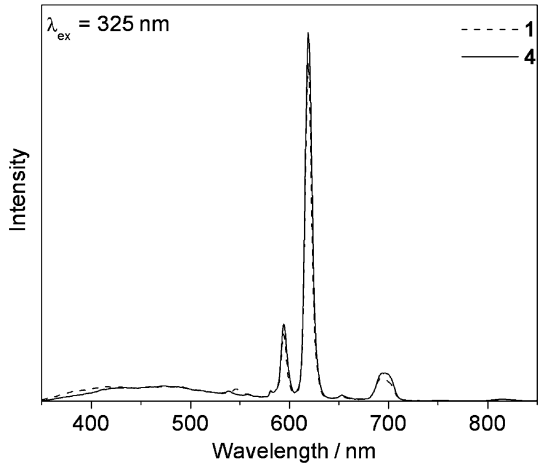

Figure 9. Solid-state normalized emission spectra for Eu complexes **1** and **4** (10 K), λ_{ex} = 325 nm.

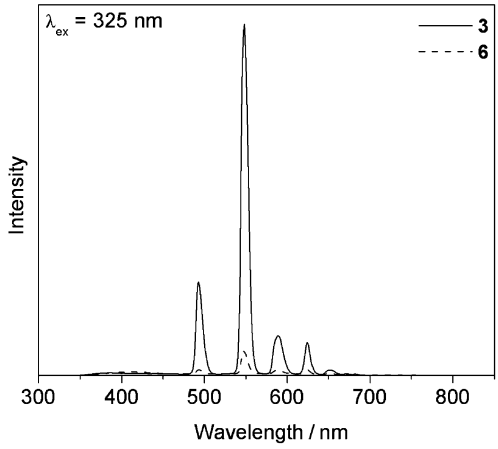

Figure 10. Solid-state normalized emission spectra for Tb complexes **3** and **6** (10 K), λ_{ex} = 325 nm.

Table 1. The solid-state luminescence lifetime (τ) and quantum yield (Φ) of the ligands and lanthanide complexes at 10 K. (λ_{ex} = 337 nm, **L¹** λ_{em} = 405 nm, **L²** λ_{em} = 410 nm, **1** and **4** λ_{em} = 616 nm, **2** and **5** λ_{em} = ca. 450 nm, **3** and **6** λ_{em} = 545 nm).

	L¹	**L²**	**1**	**2**[a]	**3**	**4**	**5**[a]	**6**
τ [ms]	9.1×10^{-6}	17.6×10^{-6}	1.29	7.67×10^{-3}	1.14	0.86	5.53×10^{-3}	1.33
Φ[b]	–	–	0.23	–	0.18	0.21	–	0.06

[a] The phosphorescence lifetimes of in **2** and **5** ($\mathbf{T_1}\rightarrow \mathbf{S_0}$) are measured at 10 K.[15] [b] Quantum yield obtained by comparison with sodium salicylate (as standard).[16–17]

The lowest energy level of Gd^{3+} ($^6P_{7/2}$) is much higher than energy levels of the ligands; therefore, it is assumed that there are no energy transitions between the ligand and metal.[14] The phosphorescence of these Gd complexes was measured under cold conditions (10 K) in the solid state (see Figure 8).

The luminescence lifetimes were recorded to verify the fluorescence and phosphorescence at 10 K. The emission lifetimes on a nanosecond scale ($S_1 \rightarrow S_0$) were measured at ca. 400 and 415 nm for **L¹** and **L²**, respectively, and on a microsecond scale ($T_1 \rightarrow S_0$) at ca. 440 and 470 nm for **L¹** and **L²**, respectively. The details of the luminescence lifetimes are shown in Table 1.

In line with the foregoing experimental results, the schematic energy level diagram, which includes the triplet state energy levels of the Gd complexes, and the energy transfer process are shown in Figure 11. Given that the energy level $^5D_4$ for Tb is ca. 20500 cm^{-1}, the energy gap between the ligand triplet state and the metal centre is greater than 2000 cm^{-1} in Tb complexes of ligand **L¹** , which is too high to allow an effective back transfer. In contrast, the triplet state energy levels in the Gd complexes of **L²** are too close to $^5D_4$, so is too low to prevent thermally competitive back energy transfer from the $^5D_4$ to the ligand triplet state; Hence, only a weak green f–f emission band was observed.[18]

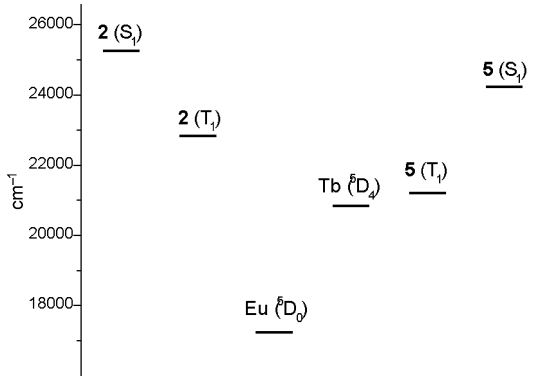

Figure 11. The lowest triplet-state energy levels of the ligands in the Gd complexes (**2** and **5**) and the resonance energy level of Eu^{3+} and Tb^{3+} ions.[19]

The energy gap between the ligand triplet states and the europium is greater than 2000 cm^{-1}, which is similar to the Tb complexes described above; however, the energy level of the $^5D_0$ state for Eu is ca. 17500 cm^{-1}, which is 3000 cm^{-1} lower than the Tb ($^5D_4$) energy level. According to the Lativa empirical rules,[19] an optimal ligand-to-metal transfer process for Eu^{3+} requires more than 2500 cm^{-1}. Comparison of the energy for the triplet states of **2** (22837 cm^{-1}) and **5** (21173 cm^{-1}) with that for the $^5D_0$ state for Eu (17240 cm^{-1}) suggests that the europium complexes exhibit better luminescence properties than the terbium complexes because the energy transfer from the ligands is better converted.[21]

Conclusions

Two series of lanthanide complexes coordinated with aromatic chromophore-containing pyrrole-derivatized carboxylate ligands were successfully synthesized and characterized by MS and FT-IR spectroscopic analyses. The solid-state molecular structures of some of these complexes were also precisely determined by X-ray crystallography. The X-ray diffraction studies reveal that the lanthanide complexes that incorporate bidentate carboxylate ligands (1-methylpyrrole-2-carboxylic acid and *N*-methyl-3-indoleglyoxylic acid) could attain highly symmetrical polymeric structures without any coordination with luminescence-quenching solvent or water molecules. Several europium and terbium complexes were found to be capable of exhibiting solid-state luminescence of high intensity, long lifetimes and high efficiency.

Experimental Section

General Remarks: All solvents were purified and dried by standard methods prior to use.[20] All chemicals, unless otherwise stated, were purchased commercially and used as received. Ligands 1-methylpyrrole-2-carboxylic acid (**L¹**) and *N*-methyl-3-indoleglyoxylic acid (**L²**) were acquired from commercial sources. Sodium hydroxide (1.0 equiv.) was added to a solution of **L¹** and **L²** (1.0 equiv.) in MeOH (20 mL). After stirring the solution for about 1 h at room temperature, lanthanide(III) nitrate hexahydrate (Ln = Eu, Gd and Tb) (1.0 equiv.) was added to the reaction mixture. The resulting reaction mixture was then stirred at room temperature for another 24 h. The precipitate that was formed was isolated by suction filtration and purified by washing with CH_2Cl_2 and MeOH. The purified product was finally isolated as a powder.

[(1-Methylpyrrole-2-carboxylate)$_3$Eu]$_n$ (1): 1-Methylpyrrole-2-carboxylic acid (150 mg) was used as the chelating ligand, and the purified product was isolated as a dark brown powder. Yield: 349 mg (56%). MS (ESI, MeOH): *m*/*z* = 526 [M^+ + 2], 525 [M^+ + 1], 524 [M^+], 523 [M^+ – 1]. IR (KBr): $\tilde{\nu}$ = 1560 and 1545 [asymmetric $\nu(COO^-)$], 1458 [symmetric $\nu(COO^-)$] cm^{-1}. $C_{18}H_{18}EuN_3O_6$ (534.2): calcd. C 41.23, H 3.46, N 8.01; found C 41.22, H 3.45, N 8.05.

[(1-Methylpyrrole-2-carboxylate)$_3$Gd]$_n$ (2): 1-Methylpyrrole-2-carboxylic acid (150 mg) was used as the chelating ligand, and the purified product was isolated as a dark brown powder. Yield: 360 mg (57%). MS (ESI, MeOH): *m*/*z* = 534 [M^+ + 4], 533 [M^+ + 3], 532 [M^+ + 2], 531 [M^+ + 1], 530 [M^+], 529 [M^+ – 1], 528 [M^+ – 2]. IR (KBr): $\tilde{\nu}$ = 1560 and 1545 [asymmetric $\nu(COO^-)$], 1458 and 1425 [symmetric $\nu(COO^-)$] cm^{-1}. $C_{18}H_{18}GdN_3O_6$ (529.6): calcd. C 40.82, H 3.43, N 7.93; found C 40.83, H 3.46, N 7.91

[(1-Methylpyrrole-2-carboxylate)$_3$Tb]$_n$ (3): 1-Methylpyrrole-2-carboxylic acid (150 mg) was used as the chelating ligand, and the purified product was isolated as a dark brown powder. Yield: 318 mg (50%). MS (ESI, MeOH): *m*/*z* = 531 [M^+], 530 [M^+ – 1], 529 [M^+ – 2]. IR (KBr): $\tilde{\nu}$ = 1541 [asymmetric $\nu(COO^-)$], 1466 and 1429 [symmetric $\nu(COO^-)$] cm^{-1}. $C_{18}H_{18}N_3O_6Tb$ (521.2): calcd. C 40.69, H 3.41, N 7.91; found C 40.66, H 3.46, N 7.90.

[(*N*-Methyl-3-indoleglyoxylate)$_2$Eu(NO$_3$)(MeOH)$_2$]$_n$ (4): *N*-Methyl-3-indoleglyoxylic acid (200 mg) was used as the chelating ligand, and the purified product was isolated as a bright greenish-yellow powder. Yield: 346 mg (52%). MS (ESI, MeOH): *m*/*z* = 683 [M^+ + 1], 682 [M^+], 681 [M^+ – 1], 680 [M^+ – 2]. IR (KBr): $\tilde{\nu}$ = 3700–2700 [ν(O–H)(coordinated MeOH)], 1636 [ν(C=O)], 1576 [asymmetric $\nu(COO^-)$], 1466 [ν(N–O)(coordinated)], 1437 and 1405 [symmetric $\nu(COO^-)$], 1254 [ν(N–O)(coordinated)], 1091 [ν(N–O)(coordinated)] cm^{-1}. $C_{25}H_{28}EuN_3O_{12}$ (714.4): calcd. C 42.03, H 3.95, N 5.88; found C 42.01, H 3.96, N 5.87.

[(*N*-Methyl-3-indoleglyoxylate)$_2$Gd(NO$_3$)(MeOH)$_2$]$_n$ (5): *N*-Methyl-3-indoleglyoxylic acid (200 mg) was used as the chelating ligand, and the purified product was isolated as a bright greenish-yellow powder. Yield: 342 mg (51%). MS (ESI, MeOH): *m*/*z* = 691 [M^+ + 3], 690 [M^+ + 2], 689 [M^+ + 1], 688 [M^+], 687 [M^+ – 1], 686 [M^+ – 2], 685 [M^+ – 3]. IR (KBr): $\tilde{\nu}$ = 3700–2700 [ν(O–H)(coordinated MeOH)], 1637 [ν(C=O)], 1576 [asymmetric $\nu(COO^-)$], 1466 [ν(N–O)(coordinated)], 1431 and 1405 [symmetric $\nu(COO^-)$], 1252 [ν(N–O)(coordinated)], 1091 [ν(N–O)(coordinated)] cm^{-1}. $C_{25}H_{28}GdN_3O_{12}$ (719.7): calcd. C 41.72, H 3.92, N 5.84; found C 41.73, H 3.96, N 5.81.

[(*N*-Methyl-3-indoleglyoxylate)$_2$Tb(NO$_3$)(MeOH)$_2$]$_n$ (6): *N*-Methyl-3-indoleglyoxylic acid (200 mg) was used as the chelating ligand, and the purified product was isolated as a bright greenish-yellow powder. Yield: 323 mg (48%). MS (ESI, MeOH): *m*/*z* = 689 [M^+], 688 [M^+ – 1], 687 [M^+ – 2]. IR (KBr): $\tilde{\nu}$ = 3700–2700 [ν(O–H)(coordinated MeOH)], 1637 [ν(C=O)], 1574 [asymmetric $\nu(COO^-)$], 1466 [ν(N–O)(coordinated)], 1431 and 1405 [symmetric $\nu(COO^-)$], 1253 [ν(N–O)(coordinated)], 1090 [ν(N–O)(coordinated)] cm^{-1}. $C_{25}H_{28}N_3O_{12}Tb$ (721.4): calcd. C 41.62, H 3.91, N 5.82; found C 41.63, H 3.96, N 5.81.

Crystallography Data: Single crystals that were suitable for X-ray crystallographic analyses of complexes **1** and **4** were mounted in glass capillaries. Diffraction data were collected at room temperature with a Bruker AXS SMART CCD diffractometer equipped with graphite-monochromated Mo-K_α radiation (λ = 0.71073 Å). Crystallographic collection data and structure refinements are summarized in Table 2. Intensity data were also corrected for Lorentz and polarisation effects, and an approximation of absorption correction by inter-image scaling was applied. The space groups of both crystals were determined from a combination of Laue symmetry checks, and their systematic absences were confirmed by successful refinement of the structures. The structures were solved by direct methods, SIR 92[22] or SHELXS 97,[23] along with Fourier-difference techniques. Structural refinements were made on *F* by full-matrix least-squares analysis. The hydrogen atoms of the organic moieties were generated in their idealized position. All calculations were performed on a personal computer by using the program package CrystalStructure.[24] CCDC-600404 and -641121 contain the supplementary crystallographic data for this paper. These data can be obtained free of charge from The Cam-

Table 2. Crystal data and structure refinement parameters for **1** and **4**.

	1	**4**
Empirical formula	$C_{18}H_{18}EuN_3O_6$	$C_{25}H_{28}EuN_3O_{12}$
Formula weight	524.32	714.47
Crystal color, habit	light yellow, rod	light yellow, plate
Crystal dimensions [mm]	0.04 × 0.05 × 0.42	0.08 × 0.32 × 0.46
Crystal system	monoclinic	monoclinic
Lattice type	primitive	primitive
Space group	$P2_1/c$ (#14)	$P2_1/c$ (#14)
a [Å]	12.273(2)	25.764(6)
b [Å]	21.604(4)	10.352(2)
c [Å]	7.586(1)	10.735(2)
β [°]	97.47(1)°	94.720(10)
V [Å^3]	1994.3(6)	2853.4(10)
Z	4	4
$D_{calcd.}$ [g cm^{-3}]	1.746	1.663
$2\theta_{max}$ [°]	55	55
F(000)	1032	1432
μ (Mo-K_α) [cm^{-1}]	31.77	22.6
Number of reflections measured	24400	17621
Number of unique reflections	4567	6717
$R_{int.}$	0.024	0.039
Number of observed reflections [$I > 2\sigma(I)$]	3068	5249
Number of parameters	268	408
R[a]	0.025	0.028
R_w[b]	0.029	0.062
Goodness of fit (GOF)[c]	1.051	1.042
Max. shift / error	0	0.02

[a] $R = [\Sigma(||F_o| - |F_c||)] / \Sigma|F_o|$. [b] $R_w = [\Sigma w(|F_o| - |F_c|)^2 / \Sigma w|F_o|^2]^{1/2}$. [c] GOF = $[\Sigma w(|F_o| - |F_c|)^2 / (N_{obs} - N_{param})]^{1/2}$.

bridge Crystallographic Data Centre via www.ccdc.cam.ac.uk/data_request/cif.

Photophysical Measurements: The UV/Vis absorption spectra were recorded by using a HP UV-8453 spectrophotometer to measure the range between 200 and 1100 nm in MeOH (10^{-3} M). The solution-state excitation spectra were recorded by using a Perkin–Elmer LS 50B Luminescence spectrophotometer that was equipped with a R928 photomultiplier tube, and the spectra were corrected for detector response and stray background light. The solid samples were housed in an Oxford (CC1104) instruments closed-cycle cryostat pulsed by cryodrive (Edwards 1.5) for luminescence spectra collected at 10 K. The temperature was adjusted from 10 K to 300 K by using a programmable intelligent temperature controller (Oxford IT502). A He–Cd laser (Kimmon IK5352R-D) at 325 nm with a maximum power of 5 mW was used. The excitation light was modulated at 20 Hz by using a mechanical chopper (Stardford SR540). The emitted light from the sample was then collected and detected by using a 25-mm focal length double monochromator with a thermoelectrically cooled photomultiplier tube (PMT) (Hamamatsu R363–10) as the detector. For lifetime measurements, the 337-nm pulsed line from a nitrogen laser was used as the excitation light. The sample was pulsed by this light source with a 4-ns pulse width. The decay-time spectra were examined by a HP5452A 500 MHz oscilloscope.[15]

Supporting Information (see footnote on the first page of this article): Selected bond lengths and angles for **1** and **4**; solid-state emission spectra of the ligands $\mathbf{L^1}$ and $\mathbf{L^2}$.

Acknowledgments

The authors acknowledge the financial support of the Hong Kong Research Grants Council, City University of Hong Kong and the University of Hong Kong. G. L. L. acknowledges the receipt of a postgraduate studentship administered by the University of Hong Kong, and K. L. W. acknowledges the Research Scholarship Enhancement Scheme of the City University of Hong Kong.

[1] S. P. Fricker, *Chem. Soc. Rev.* **2006**, *6*, 524–533.
[2] A. Beerby, L. M. Bushby, D. Maffeo, J. A. G. Williams, *J. Chem. Soc. Dalton Trans.* **2002**, 48–54.
[3] K.-L. Wong, W.-M. Kwok, W.-T. Wong, D. L. Phillips, K.-W. Cheah, *Angew. Chem. Int. Ed.* **2004**, *43*, 4659–4662.
[4] G. F. de Sá, O. L. Malta, C. Mello Donegá, A. M. Simas, R. L. Longo, P. A. Santa-Cruz, E. F. da Silva Jr., *Coord. Chem. Rev.* **2000**, *196*, 165–195.
[5] H. C. Aspinal, *Chem. Rev.* **2002**, *102*, 1807–1850.
[6] A. de Bettencourt-Dias, A. Poloukhtine, *J. Phys. Chem. B* **2006**, *110*, 25638–25645; S. Visaanathan, A. de Bettencourt-Dias, *Inorg. Chem.* **2006**, *45*, 10138–10146; D. Parker, R. S. Dickins, H. Puschmann, C. Crossland, J. A. K. Howard, *Chem. Rev.* **2002**, *102*, 1977–2010.
[7] J. Zhang, P. D. Badger, S. J. Geib, S. Petoud, *Angew. Chem. Int. Ed.* **2005**, *44*, 2508–2512.
[8] J.-C. G. Bunzli, C. Piguet, *Chem. Rev.* **2002**, *102*, 1897–1928.
[9] H. Tsukube, S. Shinoda, *Chem. Rev.* **2002**, *102*, 2389–2404.
[10] I. Lukeš, J. Kotek, P. Vojtıšek, P. Hermann, *Coord. Chem. Rev.* **2001**, *216–217*, 287–312.
[11] W. P.-W. Lai, W.-T. Wong, B. K.-F. Li, K.-W. Cheah, *New J. Chem.* **2002**, *26*, 576–581.
[12] A. W.-H. Lam, W.-T. Wong, S. Gao, G.-H. Wen, X.-X. Zhang, *Eur. J. Inorg. Chem.* **2003**, 149–163.
[13] J. Sztucki, W. Stręk, *Chem. Phys.* **1990**, *143*, 347–357.
[14] J.-C. G. Bunzli, "Spectroscopic Properties of Rare Earths" in *Optical Materials* (Ed.: G. K. Liu), Springer-Verlag, Berlin, **2002**.
[15] L. D. Carlos, J. A. Fernandes, R. A. Sá Ferreira, O. L. Malta, I. S. Gonçalves, P. Ribeiro-Claro, *Chem. Phys. Lett.* **2005**, *413*, 22–24.
[16] R. Pavithran, M. L. P. Reddy, S. A. Junior, R. O. Freire, G. B. Rocha, P. P. Lima, *Eur. J. Inorg. Chem.* **2005**, 4129–4137.
[17] M. Latva, H. Takalo, V. M. Mukkala, C. Matachescu, J. C. Rodríguez-Ubis, J. Kankare, *J. Lumin.* **1997**, *75*, 149–169.
[18] G. R. Choppin, D. R. Peterman, *Coord. Chem. Rev.* **1998**, *174*, 283–299.
[19] M. Shi, F. Li, T. Yi, D. Zhang, H. Hu, C. Huang, *Inorg. Chem.* **2005**, *44*, 8929–8936.
[20] A. Dadabhoy, S. Faulkner, P. G. Sammes, *J. Chem. Soc., Perkin Trans. 2* **2002**, 348–357.
[21] D. D. Perrin, W. L. F. Armarego, *Purification of Laboratory Chemicals*, Pergamon, Oxford, 4th ed., **1996**.
[22] *SIR 92*: A. Altomare, G. Cascarano, C. Giacovazzo, A. Guagliardi, M. C. Brula, G. Polidori, M. Camalli, *J. Appl. Crystallogr.* **1994**, *27*, 435.
[23] G. M. Sheldrick, *SHELXS 97*, University of Göttingen, Germany, **1997**.
[24] *CrystalStructure*, Single Crystal Structure Analysis Software, version 3.5.1, Rigaku/MSC Corporation, Rigaku/MSC, 9009 New Trails Drive, The Woodlands, Texas, USA, Rigaku, Akishima, Tokyo, Japan, **2003**; D. J. Watkin, C. K. Prout, J. R. Carruthers, P. W. Betteridge, *Crystals*, Chemical Crystallography Lab., Oxford, UK, **1996**, issue 10.

Received: June 5, 2007
Published Online: October 17, 2007

